J. Plasma Fusion Res. SERIES, Vol. 6 (2004) 647–650

Mechanisms of Plasma Production Using Folded Waveguide Antenna

TORII Yuki, KUMAZAWA Ryuhei[1], WATARI Tetsuo[1], MUTOH Takashi[1], SEKI Tetsuo[1], SAITO Kenji[1], TAKEUCHI Norio[2], WATANABE Tsuguhiro[1], SHIMPO Fujio[1], NOMURA Goro[1], KATOH Akemi[1], ZHAO Yangping[3] and LHD Experimental Group[1]

Institute of Advanced Energy, Kyoto University, Uji 611-0011, Japan

[1]National Institute for Fusion Science, Toki 509-5292, Japan

[2]Nagoya University, Energy Engineering and Science, Nagoya 464-8601, Japan

[3]Institute of Plasma Physics, Academia Sinica, 230031, Hefei, Anhui, China

(Received: 9 December 2003 / Accepted: 11 August 2004)

Abstract

Wave propagation and absorption of the wave power in an initial phase of plasma production by a folded waveguide antenna installed in the Large Helical Device were investigated by a ray tracing method. The calculated ray trajectory showed that a surface electrostatic wave propagates in a low-density and low-temperature plasma in the initial plasma production phase. Then a shear Alfvén wave can propagate at a relatively higher density. The power absorption occurs through a collisional damping process in a wide range of density and at electron temperatures lower than 100 eV. Thus, propagation of a surface electrostatic wave and collisional damping seem to play important roles in the plasma production.

Keywords:

plasma production, LHD, folded waveguide antenna, ICRF, shear Alfvén wave, surface electrostatic wave

1. Introduction

On the Large Helical Device (LHD), a plasma production experiment using a folded waveguide (FWG) antenna was carried out. The FWG antenna is a waveguide antenna folded many times to lower the cutoff frequency to the ion cyclotron range of frequency (ICRF) [1]. The FWG antenna was installed in the LHD. A plasma with an electron density of 3×10^{18} m^{-3} was produced using the antenna, which was being applied to the torus device for the first time [2]. The achieved electron density was increased placing the FWG antenna nearer the plasma. These phenomena were explained in terms of the propagation area of shear Alfvén wave (SAW). In this paper, the plasma production process of this experiment is reported. Employing a ray tracing method, ray trajectories of waves in ICRF and the power absorption process were investigated.

2. Ray tracing calculation

The plasma production process was investigated with the ray tracing method. It is a simple calculation method for investigating wave propagation and the damping process [3]. Time derivatives for a position vector $\vec{r}$ and a wave number vector $\vec{k}$ are expressed in the following equations:

$$\frac{\mathrm{d}\vec{r}}{\mathrm{d}t} = -\frac{\partial D_r}{\partial \vec{k}} \Big/ \frac{\partial D_r}{\partial t} \tag{1}$$

$$\frac{\mathrm{d}\vec{k}}{\mathrm{d}t} = \frac{\partial D_r}{\partial \vec{r}} \Big/ \frac{\partial D_r}{\partial t} \tag{2}$$

where D_r, t, and ω are a real part of a dispersion relation of wave, time, and an angular frequency of the wave, respectively. Here, the following dispersion relation D in hot plasma with elements of a dielectric tensor [4], K_{xx}, K_{xy}, … , K_{zz}, was used:

$$D = \begin{vmatrix} K_{xx} - N_\parallel^2 & K_{xy} & K_{xz} + N_\perp N_\parallel \\ K_{yx} & K_{yy} - N^2 & K_{yz} \\ K_{zx} + N_\perp N_\parallel & K_{zy} & K_{zz} - N_\perp^2 \end{vmatrix} \tag{3}$$

where N is a refractive index. Subscripts "∥" and "⊥" denote parallel and perpendicular components to the magnetic field line, respectively. A damping of the wave power is calculated integrating an inner product of the imaginary part of wave number vector $\vec{k}_i$ and the position vector along the ray trajectory. If the imaginary part of the dispersion relation D_i

Corresponding author's e-mail: torii@center.iae.kyoto-u.ac.jp

is much smaller than the real part, the integration is changed over time as shown in the following equation:

$$\frac{P}{P_0} = \exp\left(-2\int \vec{k}_i \cdot \mathrm{d}\vec{r}\right) = \exp\left(-2\int D_i / \frac{\partial D_r}{\partial \omega}\mathrm{d}t\right) \quad (4)$$

In this calculation, the right hand side of the above equation is used.

3. Calculated ray trajectory

A result of ray tracing calculation of the shear Alfvén wave is shown in Fig. 1. In this calculation the following parameters, which are ones obtained in the plasma production experiment, are used: B_{ax} = 2.6 T, f = 25.33 MHz, n_{e0} = 2.0 × 10^{18} m^{-3}, and T_{e0} =20 eV. Profiles of the plasma temperature and the density are $T_e = T_i = T_{e0}\,(1-\rho^2)$ and $n_e = n_i = n_{e0}\,(1-\rho^8)$, respectively, where ρ is the normalized minor radius. A ray of SAW with $k_{\parallel}$ = 6 m^{-1}, which is deduced from the width of the FWG antenna, was started at (x, y, z) = (0.0 m, 4.3 m, 0.0 m) (ρ = 0.96). The ray travels along the magnetic lines of force and gradually penetrates into the plasma core region. Figure 2(a) shows propagation areas of SAW in the cold plasma. The parallel wave number is kept constant. Here, the propagation area is defined calculating the square of the perpendicular refractive index to be positive, i.e., $N_{\perp}^2 > 0$. The wave propagates in the area between L cutoff layer and Alfvén resonance layer, which is a hatched area. In this condition, the ray travels within the propagation region.

In the case of a little lower density, n_{e0} = 1.5 × 10^{18} m^{-3}, a ray trajectory calculated with the same parameters in Fig. 1 except for the electron density is shown in Fig. 3. The propagation area of SAW is shown in Fig. 2(b). In this case as well, the ray, which has started at the points between L cutoff layer and Alfvén resonance layer, proceeds along the magnetic field. However, the ray travels to the central region beyond the L cutoff layer, which is the region denoted by "SEW" in Fig. 2(b). It is noted that SAW converts into surface electrostatic wave (SEW) near the L cutoff layer. It is confirmed that the calculated wave number and frequency satisfies a dispersion relation of SEW [5]:

$$N_{\perp}^2 = \frac{S - N_{\parallel}^2}{\dfrac{S}{P} + \dfrac{\omega_{pi}^2 v_{ti}^2}{2\omega_{ci}^2 c^2}\left(\dfrac{\omega^2}{\omega_{ci}^2-\omega^2} - \dfrac{\omega^2}{4\omega_{ci}^2-\omega^2}\right)} \quad (5)$$

where S and P are the Stix dielectric tensor elements in cold plasma and ω_{pi}, ω_{ci}, v_{ti}, and c are the plasma frequency, the cyclotron frequency, the thermal velocity of ions, and the light velocity, respectively.

In the lower density plasma in which no SAW propagation region exists, it is deduced that SEW directly excited by the FWG antenna propagates. In this experimental condition, not the kinetic Alfvén wave, but the SEW propagates in the lower plasma temperature. Thus, it is assumed that SEW propagation and the power absorption play an important role in the plasma production phase.

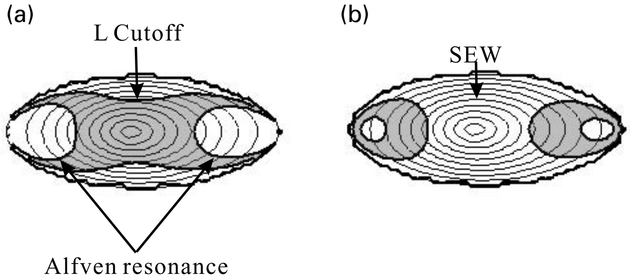

Fig. 2 Propagation areas of SAW on the horizontal elongated plane of LHD. In this calculation, a dispersion relation of cold plasma was used. SAW propagates between the L cutoff layer and the Alfvén resonance layer (hatched area). The following parameters were used: B_{ax} = 2.6T, $k_{\parallel}$ = 6 m^{-1}, f = 25.33 MHz, and $n_e = n_i = n_{e0}(1-\rho^8)$. Central densities are (a) n_{e0} = 2.0 × 10^{18} m^{-3} and (b) n_{e0} = 1.5 × 10^{18} m^{-3}, respectively. Region denoted by "SEW" are propagation areas of surface electrostatic wave.

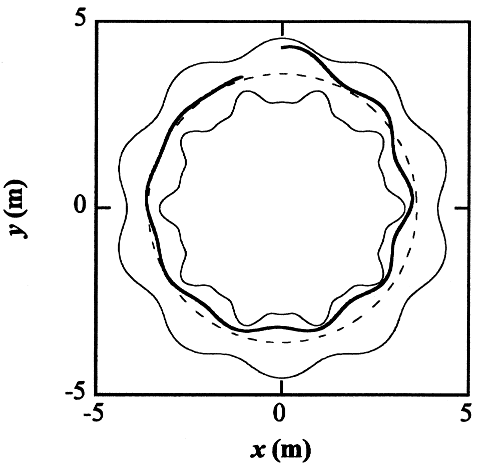

Fig. 1 Calculated ray trajectory. In this calculation, B_{ax} = 2.6 T, n_{e0} = 2.0 × 10^{18} m^{-3}, and T_{e0} = 20 eV were used. A ray with $k_{\parallel}$ = 6 m^{-1} started at (x, y, z) = (0.0 m, 4.3 m, 0.25 m). The calculation was carried out for 20,000 steps.

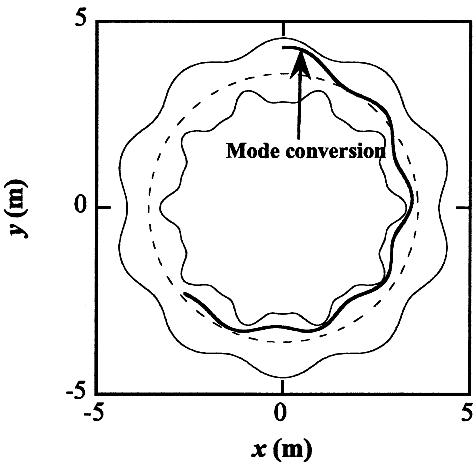

Fig. 3 Calculated ray trajectory. In this calculation, B_{ax} = 2.6 T, n_{e0} = 1.5 × 10^{18} m^{-3}, and T_{e0} = 20 eV were used. A ray with $k_{\parallel}$ = 6 m^{-1} started at (x, y, z) = (0.0 m, 4.3 m, 0.25 m). The calculation was carried out for 20,000 steps. At the point "Mode conversion", SAW changes into SEW.

4. Absorption process of wave energy

4.1 Collisionless plasma:

Varying the temperature T_{e0} and the electron density n_{e0} on the axis, the ratio of the absorbed power after traveling around the torus to the injected power was assessed and shown in Fig. 4. In the range of density, 7.0×10^{16} m^{-3} n_{e0} 7.0×10^{17} m^{-3}, power absorption does not occur in the lower temperature, below 50 eV. As the temperature exceeds 100 eV, the electron Landau damping (ELD) comes to play an important role for the power absorption. When the temperature is about 500 eV, almost all the wave power is absorbed while the ray travels around the torus. In the phase of plasma production in which the temperature is less than 50 eV it is concluded that the plasma heating through the ELD does not occur. In this calculation, the plasma is assumed to be collisionless, so that collisional heating processes seem to be important in the plasma production.

4.2 *e*-H$^+$ collision plasma:

Power absorption in the collisional plasma was estimated in the following way: A dielectric tensor **K** consists of a unit tensor **I** and a conductivity tensor σ. Moreover, σ is the sum of an electron conductivity tensor σ_e and an ion conductivity tensor σ_i,

$$\mathbf{K} = \mathbf{I} + \frac{1}{i\omega}\sigma(\omega) = \mathbf{I} + \frac{1}{i\omega}\sigma_e(\omega) + \frac{1}{i\omega}\sigma_i(\omega) \qquad (6)$$

In this calculation, it is assumed that only electron collision, with collision frequency ν, occurs. The effect of collision is considered by replacing ω by $\omega + i\nu$ in the electron conductivity tensor σ_e,

$$\mathbf{K} = \mathbf{I} + \frac{1}{i\omega}\sigma_e(\omega + i\nu) + \frac{1}{i\omega}\sigma_i(\omega) \qquad (7)$$

Assuming a process in which electrons collide with field ions, an absorbed power of the wave is calculated. In the range of density, 7.0×10^{16} m^{-3} n_{e0} 7.0×10^{17} m^{-3}, the power absorption due to the collisional damping process increased with a decrease in the temperature to lower than 100 eV. In the case of the temperature near 1 eV, almost all the wave power is absorbed while the ray proceeds around the torus. Besides, in the case of the higher density, absorption occurs at a higher temperature.

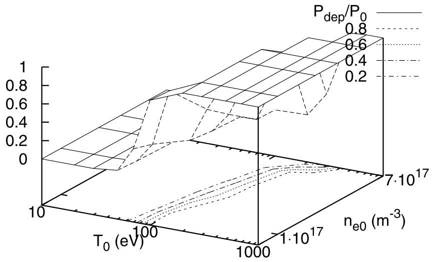

Fig. 4 The dependence of power absorption ratio on central plasma temperature T_0 and central density n_{e0}. The ratio of absorbed power after the ray travels around torus to initial wave power is shown. A contour map of it is shown on the T_0–n_{e0} plane. A collisionless plasma is assumed. Here, electron Landau damping occurs.

4.3 *e*-H^0 collision plasma:

At a lower electron density, one less than $n_{e0} = 10^{17}$ m^{-3}, the *e*-H$^+$ collisional damping becomes less effective. Therefore in the phase of the plasma production, a collision process between electrons and neutral atoms of hydrogen, H^0 should be considered. Absorbed power through *e*-H^0 collisional damping was calculated and is shown in Fig. 5. In this calculation, the collision frequency was determined from the cross-section of the collision [6]. The calculation is carried out in the range of 10 eV T_{e0} 1 keV and 7×10^{16} m^{-3} n_{e0} 7×10^{17} m^{-3}. The density of hydrogen atoms is assumed to be $n_{H0} = n_{0H^0} - n_e = n_{0H^0} - n_i$. The density of hydrogen atoms when no atoms are ionized, n_{0H^0}, is 4.0×10^{18} m^{-3}, which is deduced from the gas-puffing amount, the gas temperature, and the LHD vacuum vessel volume. In case of T_{e0} < 50 eV where no Landau damping occurs, 10 – 20 percent of the wave power is absorbed over a wide range of density. On the other hand, at temperatures above 200 eV almost all wave power is absorbed through the ELD while the ray goes around the torus.

4.4 *e*-H$_2$ collision plasma:

In the initial phase of plasma production, collisions between electrons and hydrogen molecules may occur. In a way similar to that discussed in the previous paragraph, the absorbed power through *e*-H$_2$ collisional damping is calculated and shown in Fig. 6 in the range of 1 eV T_{e0} 100 eV and 7×10^{15} m^{-3} n_{e0} 7×10^{17} m^{-3}. In this calculation, the cross-section of the collision described in Ref. [7] is used. The density of hydrogen molecules is represented by $n_{H_2} = n_{0H_2} - 2n_e = n_{0H_2} - 2n_i$ and n_{0H_2} is 2.0×10^{18} m^{-3}. Approximately 10 percent of wave power is damped in the case of temperatures and densities where no Landau damping occurs, while the ray travels around the torus. However the dissociation process is higher in electron temperatures higher than 5 eV, so this absorption process may be important at lower electron temperatures.

5. Changes of the plasma production process

In previous sections, wave propagation and four power absorption processes were investigated. These results are summarized as follows:

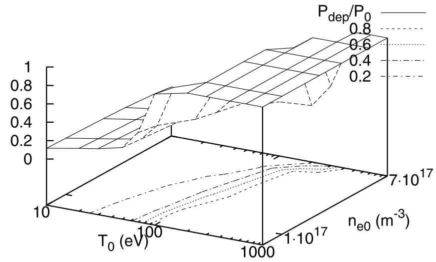

Fig. 5 The dependence of power absorption ratio on central plasma temperature T_0 and central density n_{e0}. The ratio of absorbed power through *e*-H$_0$ collisional damping after the ray travels around torus to initial wave power is shown. A contour map of it is shown on the T_0–n_{e0} plane.

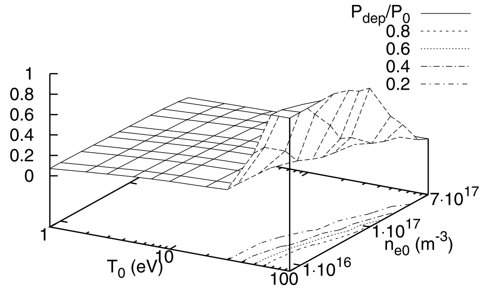

Fig. 6 The dependence of power absorption ratio on central plasma temperature T_0 and central density n_{e0}. The ratio of absorbed power through e-H_2 collisional damping after the ray travels around torus to initial wave power is shown. A contour map of it is shown on the T_0–n_{e0} plane.

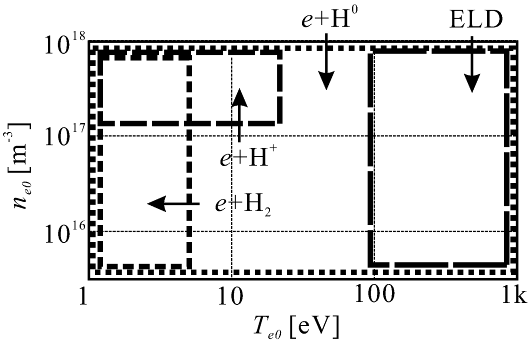

Fig. 7 The ranges of temperature and density where absorption through each process occurs.

- The SEW propagates in regions where the SAW can not propagate; it propagates between the L cutoff layer and the Alfvén resonance layer.
- In the collisionless plasma, ELD is strong when the temperature is higher than 200 eV in the parallel refractive index, $|N_{\|}| \sim 10$. In the case of temperatures lower than 50 eV, no absorption occurs.
- In the case of densities lower than 7×10^{17} m^{-3} and temperatures lower than 10 eV, e-H^+ collisional damping becomes strong. In the case of temperatures higher than 100 eV, the damping does not occur.
- e-H^0 and e-H_2 collisional damping occurs where the plasma density is lower than 7×10^{17} m^{-3} and the temperature is lower than 100 eV.

The ranges of temperature and density where absorption through each process occurs are summarized in Fig. 7.

Therefore, the following process of the wave propagation and the energy damping in the plasma production phase is deduced:

1. A few electrons in atoms are accelerated and the atoms are ionized by RF electric field near the antenna. A very low density plasma is produced and SEW propagates.
2. The energy of SEW is absorbed through collisions between electrons and hydrogen molecules. Then, the temperature rises and molecules dissociate in neutral atoms.
3. Electrons also collide with the dissociated atoms and the wave energy is absorbed. Atoms are ionized, and then electron and ion densities rise.
4. In high density plasma, shear Alfvén wave propagates.
5. At a high enough temperature, ELD dominates.

In this experiment, in which plasma temperature was not measured, it is difficult to investigate the detailed process; however, it is noted that propagation of SEW and collisional damping of the wave energy seem to play important roles in the plasma production phase.

In this research, Krook's collisional model, where a collisional term has no differentials in velocity space, was used and a collision of electrons only was assumed. For a quantitative estimation, a collisional term which has first and second order differentials and the effects of the collision of ions may be needed.

6. Summary

Using a folded waveguide antenna installed in LHD, plasma was produced. Achieved electron density was 3×10^{18} m^{-3}. Properties of the produced plasma were explained in terms of propagation of shear Alfvén wave. In order to investigate mechanisms in the plasma production phase, wave propagations and power absorption were examined by the ray tracing method. In this calculation, the hot dispersion relation was used.

The calculated ray trajectory shows that surface electrostatic wave propagates in low density plasma while shear Alfvén wave propagates in relatively high density plasma. Dependences of power deposition by different damping processes on temperature and density were calculated. ELD does not occur in low temperature plasma while collisional damping does. Plasma production mechanisms were deduced as follows: Electrons in atoms are accelerated and ionized by RF electric field near the antenna. Surface electrostatic wave propagates and the plasma is heated to high temperature and high density through collisional damping. In high density plasma, shear Alfvén wave propagates. ELD occurs at high enough temperature.

References

[1] T.L. Owens, IEEE Transaction on Plasma Science, PS-14 **6**, 934 (1986).
[2] Y. Torii *et al.*, Nucl. Fusion **42**, 679 (2002).
[3] B.D. McVey, Nucl. Fusion **19**, 461 (1979).
[4] T.H. Stix, *The Theory of Plasma Waves* (McGraw-Hill Book Co. Inc., New York, 1962) p.262.
[5] T.H. Stix, *The Theory of Plasma Waves* (McGraw-Hill Book Co. Inc., New York, 1962) p.356.
[6] P. Defrance *et al.*, J. Phys. **B 14**, 111 (1981).
[7] M. Hayashi, Institute of Plasma Physics, Nagoya University, Report No. IPPJ-AM-19 (1981).